



ISSN (E): 2277-7695

ISSN (P): 2349-8242

NAAS Rating: 5.23

TPI 2023; 12(4): 43-58

© 2023 TPI

[www.thepharmajournal.com](http://www.thepharmajournal.com)

Received: 28-02-2023

Accepted: 30-03-2023

**Ravikumar C**

Associate Professor and Head,  
Department of Veterinary  
Pharmacology and Toxicology,  
Veterinary College, Hassan,  
Karnataka, India

**Jagadeesh S Sanganal**

Professor, Department of  
Biochemistry and Toxicology,  
Institute of Animal health and  
Veterinary Biologicals, Hebbal,  
Bengaluru, Karnataka, India.

**Shridhar NB**

Professor, Department of  
Pharmacology and Toxicology,  
Veterinary College, Shivamogga,  
Karnataka, India

**Sunilchandra U**

Department of Pharmacology  
and Toxicology, Veterinary  
College, Shivamogga,  
Karnataka, India

**Ramachandra SG**

Chief Research Scientist, Central  
Animal Facility, Indian Institute  
of Science, Bengaluru,  
Karnataka, India

**Moonoshree Sarma**

Assistant Professor, Department  
of Veterinary Pharmacology and  
Toxicology, Veterinary College,  
Hassan. Karnataka, India

**Corresponding Author:****Ravikumar C**

Associate Professor and Head,  
Department of Veterinary  
Pharmacology and Toxicology,  
Veterinary College, Hassan,  
Karnataka, India

## An overview of NSAID loaded nanomaterials

**Ravikumar C, Jagadeesh S Sanganal, Shridhar NB, Sunilchandra U, Ramachandra SG and Moonoshree Sarma**

**Abstract**

Non steroidal anti-inflammatory drugs are used as analgesic antinflammatory, and antipyretic agents. Nanomaterials like nanoparticle, nanofiber, nanosuspension and nanogel used as drug delivery of NSAIDs because it improves the solubility, prolongs the duration of action and reduces the side effects of the NSAIDs. For the characterisation of the nano materials like structural characterization, particle size distribution, particle charge / zeta potential, crystalline status, scanning electron microscopy (SEM), transmission electron microscopy (TEM), dynamic light scattering, differential scanning calorimetry, X ray diffraction, FTIR etc are used. For quantification of NSAID, dissolution apparatus, HPLC and UV spectrophotometry methods are used. The *in vitro* and *in vivo* efficacy studies also conducted for the comparison of nanomaterial and conventional analgesic drugs.

Cucurbit<sup>[6]</sup>uril- Ketoprofen nanoparticles remarkably increased *in vitro* drug release and pharmacokinetic parameters like AUC, peak plasma concentration compared to compared to the conventional ketoprofen. The increase in the drug release rate, dissolution of piroxicam-PVP loaded nanofiber were increased compared with the pure drug.

The polymeric nanofiber loaded indomethacin is used in the colonic delivery of indomethacin in the treatment of colon cancer, ulcerative colitis. There will be increase in the *in vitro* skin permeation profile, anti-inflammatory effects of aceclofenac nanoemulsion compared to the conventional aceclofenac.

The nanomaterials used as drug delivery of the NSAIDs, guidelines regarding safe use of these nanomaterials in drug delivery, toxicity hazards, bioethical issues, physiological and pharmaceutical challenges will be addressed in the future and would certainly get resolved.

**Keywords:** NSAID, nanoparticle, nanofiber

**Introduction**

Non steroidal anti inflammatory drugs (NSAIDs) are heterogeneous groups of drugs having weak or mild analgesic effect with or without antipyretic and anti-inflammatory actions (Abramson *et al.*, 2001) <sup>[1]</sup>. NSAIDs produce their effect by interfering with the cyclooxygenase pathway which are involved in the biosynthesis of prostaglandins (PGs) and thromboxanes from arachidonic acid (Harmor *et al.*, 1989) <sup>[2]</sup>. NSAIDs are classified into two categories of drugs, *viz.*, Non-selective COX inhibitors and Selective COX-2 inhibitors. Both the cyclooxygenase enzymes have equal molecular weight and similar structure with the exception that the attachment site of COX-2 is greater than that of COX-1 (Lewis *et al.*, 1978; Davis *et al.*, 2000) <sup>[3, 4]</sup>.

Pharmaceutical nanotechnology is a field of science which includes application of nanoscience to pharmacy as nanomaterials, as devices like drug delivery, diagnostic, imaging and biosensor (Jain, 2007) <sup>[5]</sup>. It is focused on the design synthesis, characterization and application of materials and device on the nanoscale (Mansoori, 2005) <sup>[6]</sup>. Materials used on nano scale are polymeric nanoparticle, nanoemulsion, nanofiber, nanogel etc. (Mansoori, 2005) <sup>[6]</sup>.

**Disadvantages of conventional NSAIDs**

Conventional NSAIDs are loaded with drawbacks. These include less solubility, short half life, low bioavailability, lack of target specificity, high rate of drug metabolism, cytotoxicity and high dose requirement. They produce untoward effects on Stomach owing to inhibition of prostaglandins (PGs), which protects the gastrointestinal mucosa. The severity ranges from simple ailment like dyspepsia to peptic ulcer and gastrointestinal haemorrhage (Heyneman *et al.*, 2000; Hopper *et al.*, 2004) <sup>[7, 8]</sup>. It also causes multitude of side effects like acute renal failure, undesirable CNS effects like dizziness, allergic reactions and retention of fluid in the body (Hopper *et al.*, 2004) <sup>[8]</sup>. COX-2 inhibition affects kidney function, blood pressure, other physiological parameters etc. (Brune & Hinz, 2004; Marnett, 2009; Patrono & Rocco, 2009) <sup>[9, 10, 11]</sup>.

### Advantages of nanomaterial loaded NSAIDs

Nanotechnology is a novel technique in the field of biomedical science that helps in improving solubility and bioavailability, reducing toxicity, enhancing release and providing better formulation opportunities for drugs. Major advantages of nano-sizing include (i) enhanced solubility, (ii) improved oral bioavailability, (iii) increased rate of dissolution, (iv) increased surface area, (v) more rapid onset of therapeutic action, (vi) decreased fed/fasted variability, (vii) less amount of dose required, (viii) decreased patient-to-patient variability (ix) do not occlude blood capillaries and traverse easily to most physiological bio barrier, (x) provide effective delivery to brain and intracellular compartment (xi) protects fragile drugs/proteins from harsh biological environment and (xii) faster, safer and more accurate disease diagnosis (Jain, 2007) [15].

Nanoparticles are biocompatible biodegradable and readily soluble. These helps in maintaining the therapeutic concentration for longer time, thus reducing not only the frequency of administration but also chances of toxicity. It prolongs the half-life of drug, delivers drugs in a target to the target site. There are less Side effects and usually avoid occurrence of drug resistance (Zhang *et al.*, 2008) [12].

### Polymeric nanoparticle

Polymeric nanoparticles are solid colloidal particles measuring about 10 to 500 nm (Semete, *et al.*, 2010) [13]. Polymers suitable for preparing nanoparticles include: poly (alkylcyanocrystalates), poly (mythylidene malnolate 2.1.2), polyesters, e.g., poly (lactic acid), poly(e caprolactone), and their copolymers. Natural polymers are gelatin, albumin and alginate and Synthetic polymers are Polycaprolactone, Poly Vinyl Pyrrolidone etc (Kubik, *et al.*, 2008) [14].



**Fig 1:** Polymeric nanoparticles

### Nanofibers

These are the fibers having diameters less than 50-500 nanometers. According to National Science Foundation (NSF), these should have at least one dimension of 100 nanometer (nm) or less (Poole & Ownes, 2003) [15]. These are produced by different processes like Interfacial Polymerisation, Electro spinning And Force Spinning. Nanofibers possess special properties like low density, large surface area to mass, high pore volume and tight pore size (Heidi *et al.*, 2004). In recent times, these have gained importance in the field of healthcare systems, as a tool for drug delivery system in various diseases (Poole & Ownes, 2003) [15].

### Electrospinning

Electrospinning has occupied an important domain in the field

of nano-technology since last three decades due to the ease of fabricating nanofibers from a plethora of materials (Ramakrishna *et al.*, 2006) [16]. It is a technique widely used for manufacturing nanofibers. The process involves dissolving the drug of interest and polymer in a solvent. One should always keep in mind that the ratio of drug: polymer should be 1:4. The solution is inserted into a syringe followed by application of high voltage. On increasing the voltage, a charged jet fluid is initiated that follows a chaotic path of being stretched and bent until it reaches the grounded target. Above a critical voltage, a stable jet is formed that maintains a balance between the surface tension of the fluid and repulsive nature of the charge distribution on the surface of the fluid. The end product so formed is a three dimensional nonwoven mat of entangled nanofibers with a high surface-to-area volume (Kattamuri *et al.*, 2012) [17].

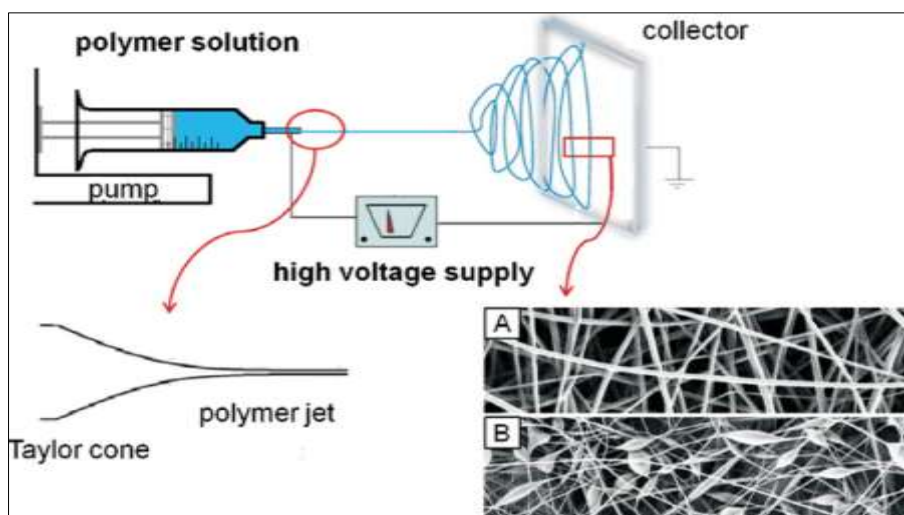


Fig 2: Electrospinning technique

### Nanoemulsion

These are a group of dispersed particles used for pharmaceutical and biomedical aids and vehicles. These are defined as transparent or translucent thermodynamically stable dispersions of oil and water stabilized by an interfacial

film of surfactant and cosurfactant molecules having a droplet size of 100nm (Shafiq *et al.*, 2007; Shafiq *et al.*, 2007) [18, 19]. These possess transdermal and dermal delivery Properties *in vitro* and *in vivo* (Kemken *et al.*, 1992; Kreilgaard, 2001) [20, 21].

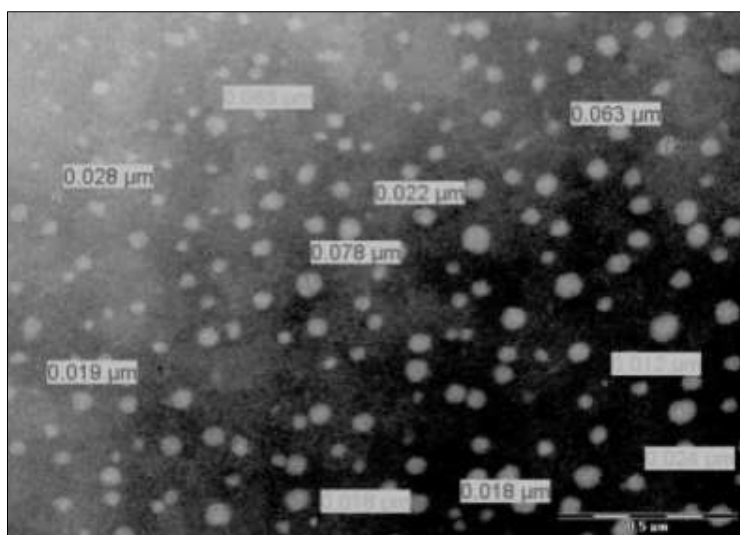


Fig 3: Nanoemulsion

### Nanogel

Gelatin is a known matrixing agent of drug delivery (Ochubiojo *et al.*, 2012) [22]. Nanoparticle composed of a hydrogel across linked hydrophilic polymer network. Nanogels are most often composed of synthetic polymers or biopolymers which are chemically or physically crosslinked. Nanogels are usually in the tens to hundreds of nanometres in diameter. Like hydrogels, the pores in nanogels can be filled with small molecules or macromolecules and their properties, such as swelling, degradation, and chemical functionality, can be controlled.

### Characterization of nanomaterials

#### Structural characterization

It is a technique used to determine the shape, size, surface morphology, structural arrangement spatial distribution,

density, geometric feature, crystal structure, quality, and orientation of nanoparticles. electronic, magnetic and thermal properties etc. Development of electron microscopy tool has improved the accessibility and feasibility in order to determine these attributes at nanometer scale. Scanning electron microscopy (SEM) provides information on structural arrangement, spatial distribution as well as surface morphology of nanoparticles.

Transmission electron microscopy (TEM) are more powerful than SEM in giving more detailed geometric features and information on quality, crystal structure and orientation of nanoparticles. Scanning tunneling microscope (STM), Atomic force microscopy (AFM) and Electrical field gradient microscopy (EFM) are used to determine the structural, electronic, magnetic and thermal properties other than the topographical properties of nanosystems (Jain, 2007) [5].





**Fig 4:** Scanning electron microscopy



**Fig 5:** Transmission electron microscopy

### Particle size distribution

Particle size distribution is also known as Polydispersity index : Polydispersity index is the degree of non uniformity of the particle size. Obviously, a low polydispersity indicates more uniform in size. As such, efforts are directed towards having a system bearing low polydispersity index. Dynamic light scattering (DLS) is a technique used to detect particles that ranges from few nanometers to about 3  $\mu\text{m}$ , while laser diffraction is largely used to measure microparticles or aggregates of drug nanoparticles. This measurement depends on the size of the particle core, the size of surface structures, particle concentration, and the type of ions in the medium (Jain, 2007) <sup>[5]</sup>.

### Particle charge / Zeta potential

It is used to know the charge at particle surface. Zeta potential optimizes formulation parameters and makes predictions pertaining to the storage stability of the colloidal dispersion. Laser doppler anemometr is the principal technique associated with zeta potential determination (Jain, 2007) <sup>[5]</sup>.

### Crystalline Status

Differential Scanning Calorimetry (DSC), X ray diffraction,

etc. are the few techniques used to assess the possible changes that occur in the physical form of drug while processing (Jain, 2007) <sup>[5]</sup>.

### NSAID quantification

The HPLC to quantify NSAID (ibuprofen). Other methods to quantify NSAIDs are dissolution apparatus and UV spectroscopy. Roullin *et al.*, (2010) <sup>[23]</sup> provided the formulas for calculating Entrapment Efficiency and Drug Loading Efficiency which are largely used to quantify NSAIDs (Roullin *et al.*, 2010) <sup>[23]</sup>.

$$EE = \frac{\text{Mass of NSAID in particles}}{\text{Mass of NSAIDs used in formulation}} \times 100$$

$$DLE = \frac{\text{Mass of NSAIDs in particles}}{\text{Mass of recovered particles}} \times 100$$

### In vitro dissolution studies

*In vitro* dissolution testing is widely used to mimic and predict *in vivo* performance of oral drug products (Lex *et al.*, 2022) <sup>[24]</sup>. To carry out *in vitro* dissolution studies, 100 mg dry powder of drug should be weighed and filled into a gelatin capsule. Round-bottomed cylindrical glass vessels having a total volume of 1000 ml are used as released chambers. The solutions should be kept in a water bath at  $37 \pm 0.5$  °C and stirred at a speed of 75 rpm. For the test in acid medium, 700 ml of HCl 0.1 N is used to obtain pH 1.2 of the release medium. For the test in base medium, 700 ml of PBS (pH 7.4) is used as release medium. Aliquot (10 ml) is withdrawn at appropriate times and immediately replaced with fresh medium equilibrated at 37 °C. The amount of released NSAID is determined by measuring UV absorption at wavelength of 258 nm. The percentage of released NSAID was determined from the following equation: (Hoai *et al.*, 2013) <sup>[25]</sup>.

$$\text{Release \%} = \frac{\text{NSAID released from the NPS}}{\text{Total amount of NSAID in NPS}} \times 100$$



Fig 6: Dissolution apparatus

#### ***In vitro* skin permeation studies**

*In vitro* skin permeation studies are performed in order to know the skin permeability of drug of interest. These are performed using Franz diffusion cell with an effective diffusional area of  $0.636 \text{ cm}^2$  and 4 mL of receiver chamber capacity using rat abdominal skin. The automated transdermal diffusion cell sampling system. 1 mL of nanoemulsion

formulation (20 mg/mL aceclofenac) or 1 g of CG (20 mg/g) was placed into each donor compartment and sealed with paraffin film to provide occlusive conditions. Samples were withdrawn at regular intervals (0.5, 1, 2, 3, 4, 5, 6, 7, 8, 9, 10, 12, 20, 22, and 24 hours), filtered through a 0.45- membrane filter, and analyzed for drug content by UV spectrophotometer at max of 274 nm (Chary *et al.*, 2011) [26].

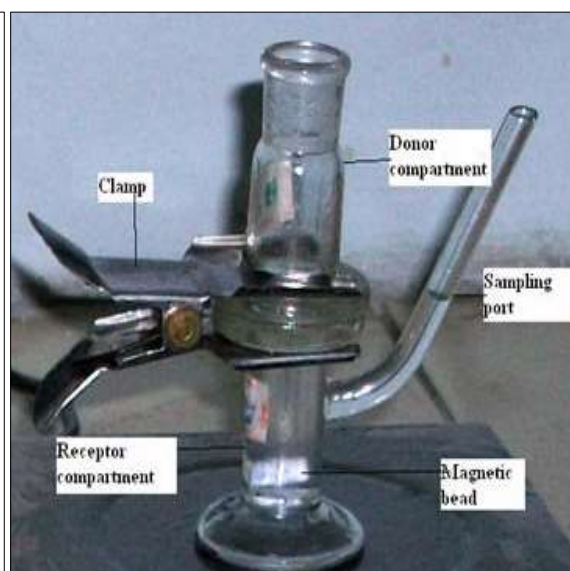
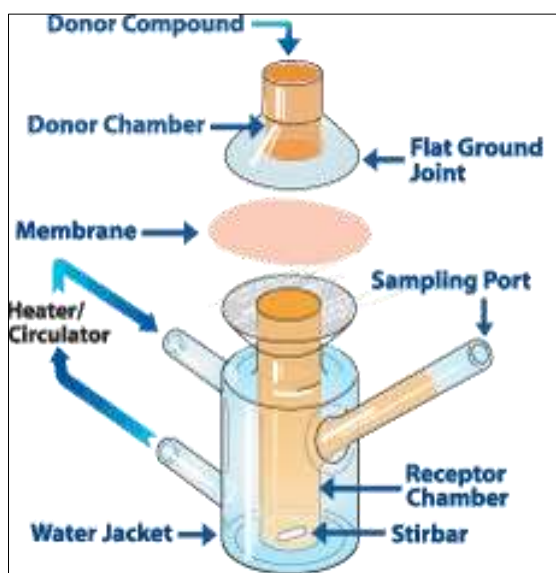


Fig 7: *In vitro* Franz diffusion cell

#### ***In vivo* assessment of oral administration**

##### ***In vivo* absorption study**

NSAID formulations were administered by oral gavages to rabbits. All rabbits are fasted 18 h prior to the dose administration and 4 h after dose administration. NSAID should be filled in a gelatin capsule and administered to rabbits by oral gavages (two capsules for each). Blood samples of 2.5 ml should be collected into vacutainer tubes containing ethylenediaminetetraacetic acid (EDTA) prior to and

0.5, 1.0, 1.5, 2.0, 2.5, 3.0, 3.5, 4.0, 6.0, 8.0, 12.0, 24.0 and 36.0 h after administration. After this collection, the blood samples are centrifuged at approximately 3500 rpm at  $2-8 \text{ }^\circ\text{C}$  for about 15 min. Each plasma specimen is collected and stored at  $-20 \text{ }^\circ\text{C}$  until analysis (Hoai *et al.*, 2013) [25].

##### ***In vivo* efficacy study**

Carrageenan-induced hind paw edema test is used in order to study the efficacy of NSAIDs *in vivo*. Paw edema is induced

by subplanter injection of carrageenan in right paw. 0.1 mL of the 1% wt/wt homogeneous suspension of carrageenan in distilled water. The volume of paw is measured at 1, 2, 3, 6, 12, and 24 h after injection using a digital plethysmometer. Percent inhibition of edema produced by each formulation treated group was calculated against the respective control group (Winter *et al.*, 1995) [27]. Results of anti-inflammatory activity were compared using the Dunnett test of 1-way ANOVA (Landucci *et al.*, 1995) [28].



Fig 8: Rat paw oedema



Fig 9: Plethysmometer

### Toxicity evaluation

Acute toxicities associated with nanosystems are enhanced endocytosis, oxidative stress and modification in protein and gene structure, while long term toxicities are bioaccumulation, poor biodistribution etc. Ex vivo toxicity evaluation generally carried out in various cell lines and MTT assay is used to determine the cell viability. *In vivo* acute and chronic toxicities are determined in various animal models. Skin irritation test and histopathology are performed to study toxicities (Jain, 2007) [5].

### Nanoparticle-NSAIDs

#### Ketoprofen encapsulated cucurbit[6]uril nanoparticles

Ketoprofen is a NSAID very often used to treat rheumatism and arthritis. But it has short half life, low bioavailability and side effects (Hoai *et al.*, 2013) [25]. Ketoprofen encapsulated cucurbit [6] uril is a nono form of ketoprofen which is prepared by solvent evaporation method. The increase in the concentration of polymer leads to gradual increase in nanoparticle diameters. This can be elaborated based on the viscosity of dispersed phase. The increasing polymer concentration is normally associated with increasing viscosity of dispersed phase. As a result, the droplet so formed is bigger in size leading to the bigger nanoparticle diameters. The control of nanoparticle sizes by changing polymer concentrations has previously been reported. This explains that the increase in polymer concentration leads to an increase in the viscous forces resisting droplet breakdown by sonication. The viscous forces oppose the shear stresses in the organic phase and the final size and size distribution of particles depends on the net shear stress available for droplet breakdown. Polymeric concentration will be directly proportional to the particle size of nanomaterial (Hoai *et al.*, 2013) [25].

### *In vitro* dissolution studies

<i>In vitro</i> release of CB[6]–Keto nanoparticles and profenid in the acidic medium (pH 1.2) <sup>a</sup> .			
Time (h)	N22 <sup>b</sup>	N25 <sup>c</sup>	Profenid <sup>d</sup>
0	0	0	0
0.5	8.4	7.8	1.7
1.0	14.1	15.2	2.1
1.5	19.7	22.1	2.9
2.0	24.6	26.9	3.4

Fig 10: Result of dissolution study in the acidic medium (pH 1.2)

### In the acidic medium (pH 1.2)

#### The results of *in vitro* release study in acidic medium of CB[6]–Keto nanoparticles and profenid

According to Hoai and co-worker, the percentages of Keto released from profenid were almost negligible (less than 5%) after 2 h. On the other hand, for the first 30 min, the percentages of Keto released from N22 and N25 were less than 10% and then gradually increased with the increasing time. However, the percentages of Keto released were nonlinear function of time. It implies that the Keto released

from CB[6]–Keto nanoparticles is due to the diffusion of Keto from the outer shells of nanoparticles or/and due to the partial dissolution of CB[6] in acidic medium. The diffusion of drugs from the outer shells of nanoparticles was confirmed earlier (Danhier *et al.*, 2009, Hu *et al.*, 2007). Keto in the outer shells was poorly entrapped in the CB[6] matrix leading to easy diffusion of Keto. Wheate and co-workers proclaimed that although CB[6] is poorly soluble in water, it still has solubility of 1–4 mM at pH 1–3 of gastric fluid resulting in the release of Keto from CB[6] matrix. However, because the

solubility of CB[6] in acidic medium is low, the percentage of released Keto is correlatively low. The above-mentioned can explain why Keto was released from nanoparticles but its

released percentage was less than 27% after 2 h in acidic medium (Hoai *et al.*, 2013) [25].

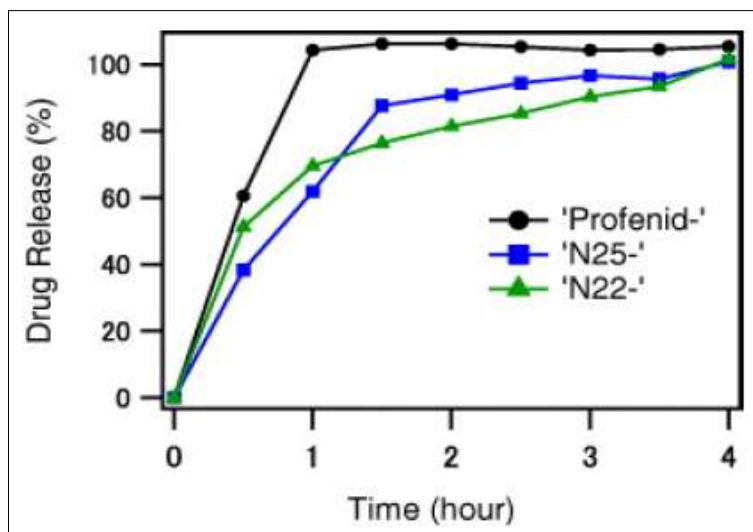


Fig 11: *In vitro* release of CB[6]-Keto nanoparticles and profenid in the acidic medium

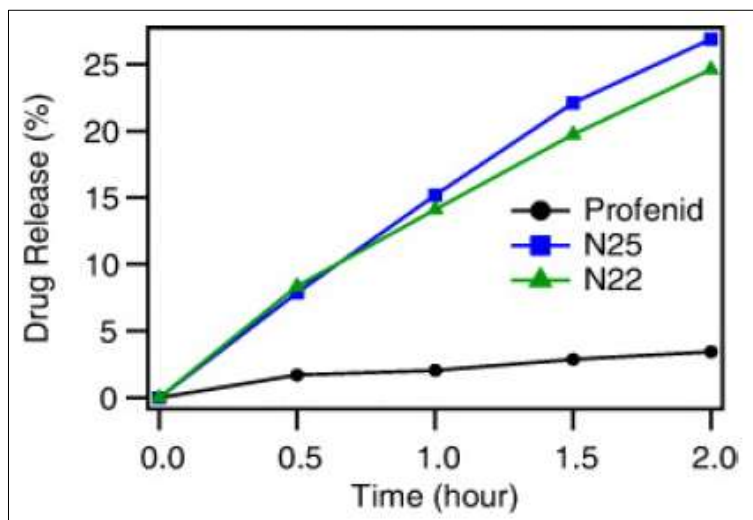


Fig 12: *In vitro* release of CB[6]-Keto nanoparticles and profenid in the basic medium

The percentages of Keto released from CB[6]-Keto nanoparticles in basic medium were significantly higher than those in acidic medium with the correlative times. For example, N22 released 38.3% of Keto at basic pH but only 8.4% of Keto at acidic pH after 30 min. This can be explained based on the solubility of CB[6] in basic medium. Also proclaimed that the solubility of CB[6] can be increased up to 45 mM in basic medium. The solubility of CB[6] is increased in the presence of cations. It forms the complexes with cations resulting in the charged complex which is hydrated more easily than the neutral molecule. The more CB[6] is

dissolved, the more Keto is released. As a result, the percentage of released Keto in basic medium was higher than that in acidic medium due to the higher solubility of CB[6] in the basic environment. Moreover, the higher percentage of released Keto in basic medium can also be explained based on the solubility of Keto in the basic environment. The carboxylic acid group in Keto is ionized in basic medium leading to increasing solubility of Keto. As a result, Keto is released readily from nanoparticles leading to increasing percentage of released Keto (Hoai *et al.*, 2013) [25].

Table 1: Pharmacokinetic parameters of keto following oral administration of CB[6]-Keto nanoparticles and Profenid

Drug formulation	Cmax <sup>b</sup> (µg ml <sup>-1</sup> )	Tmax <sup>c</sup> (h)	AUC <sup>d</sup> (µg h ml <sup>-1</sup> )	Enhance me nt ratio <sup>e</sup>
profenid	59.3	2	546.89	1.0
N25	85.9	2	692.311	1.3

<sup>a</sup>50 mg of Keto for each rabbit. <sup>b</sup>Cmax denotes maximum drug concentration <sup>c</sup>Tmax denotes time of maximum concentration <sup>d</sup>AUC area under the plasma concentration-time curve. <sup>e</sup>This is the ratio AUC of Keto/AUC of profenid.



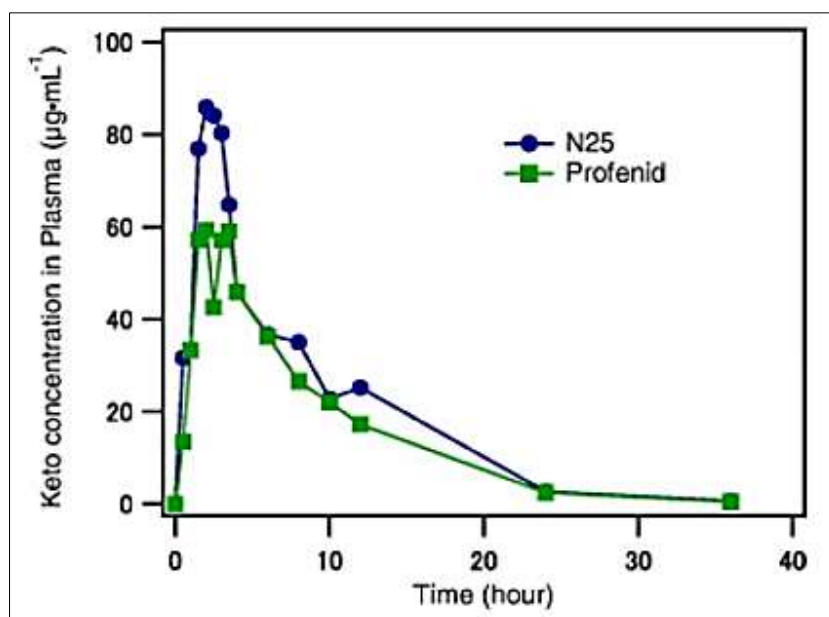


Fig 13: TEM image of Ketoprofen-loaded CB[6] particles- 100–200 nm

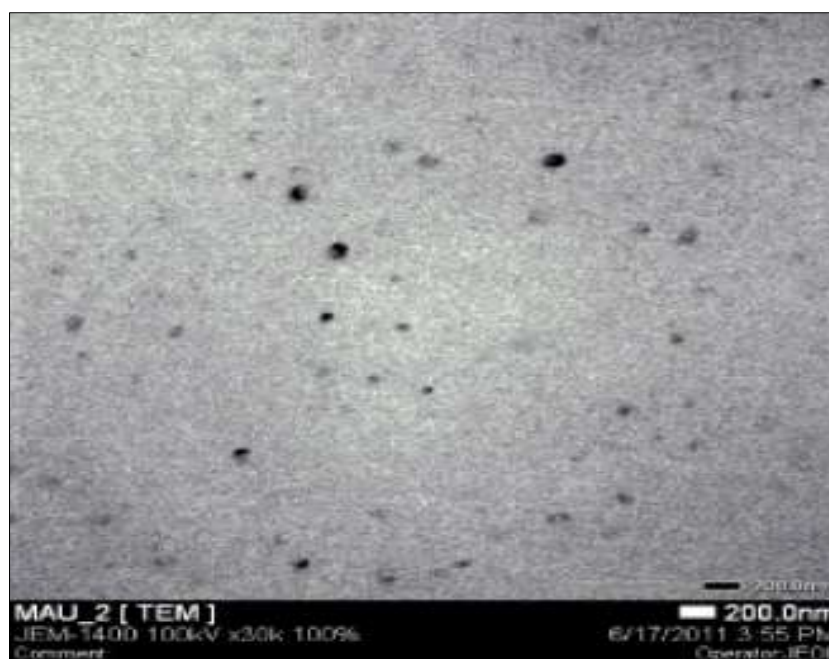


Fig 14: *In vivo* assessment of oral administration of CB[6]–Keto nanoparticles

#### Plasma concentration-time profiles of Keto after oral administration in rabbits of N25 and profenid

The *in vivo* assessment of oral administration of CB[6]–Keto nanoparticles was tested in rabbits with the aim to investigate the absorption ability of CB[6]–Keto nanoparticles, the maximum Keto concentration in plasma ( $C$ ), time of maximum concentration ( $T$ ) and the enhancement ratio of CB[6]–Ketonanoparticles. CB[6]–Keto nanoparticles and profenid were administered by oral gavages to rabbits with the amount of Keto of 50 mg for each rabbit. The oral administration procedures and the preparation of plasma are stated in section 2.4. The plasma concentration-time profiles of Keto after oral administration in rabbits are shown in figure 6. A comparison of  $T$  between N25 and profenid indicates that the concentration of Keto in plasma increased rapidly in both cases and peaks were observed after 2 h. This results imply that Keto released in the intestine from CB[6]–Keto

nanoparticles and profenid penetrated through the intestine into the bloodstream of rabbits and the  $T$  of CB[6]–Keto nanoparticles and profenid were almost the same. (Hoai *et al.*, 2013) [25]

#### Meloxicam

##### The Morphology of MLX Nanoparticles

MLX nanoparticles are obtained by the combination of anti solvent precipitation and HPH were spherical with a narrow PSD in the presence of a combination of HPMC and SDS (2:1 w/w). It was clearly seen that stabilizers were adsorbed onto the drug particle surface inhibiting particle growth and thus making the nanoparticles stable. With the formation of spherical particles it can be expected to improve powder properties of MLX, such flow ability and compressibility (Raval and Patel, 2011) [29].



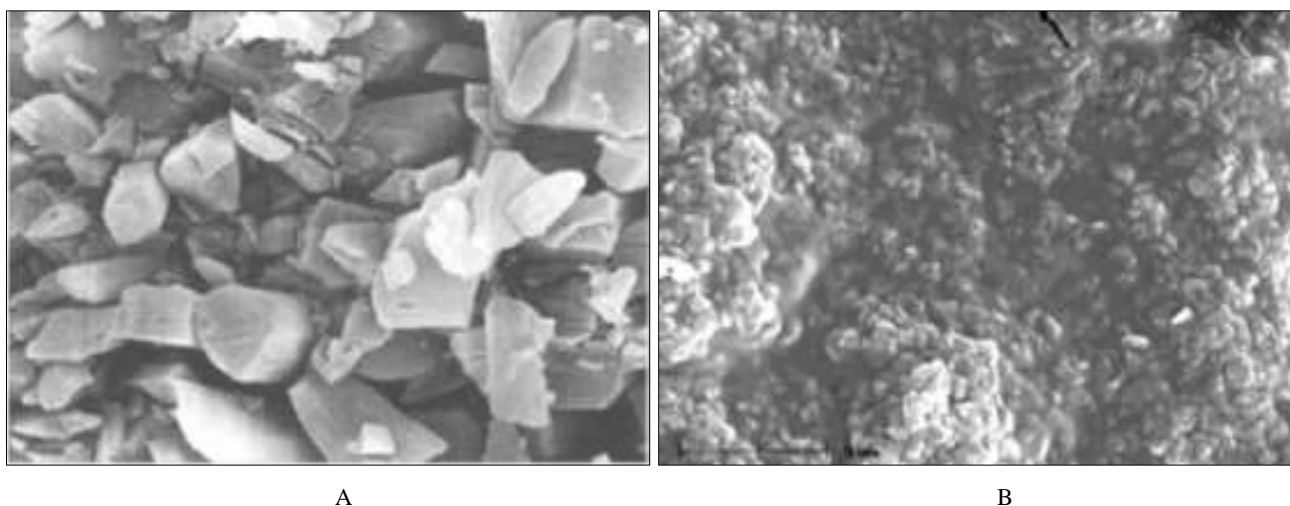


**Fig 15:** The Morphology of MLX Nanoparticles

### X-ray diffraction

The raw MLX is crystalline and exhibited crystalline peaks  $2\theta$  values from  $10$  to  $30^\circ$ , indicating crystalline nature of MLX. The MLX/stabilizer physical mixture also showed the characteristic crystalline diffraction peaks of MLX. However,

the characteristic crystalline peaks disappeared in the pattern of prepared nanoparticles producing a halo and diffused pattern typical of an amorphous material revealing that the crystallinity of MLX was decreased dramatically (Raval and Patel, 2011) [29].

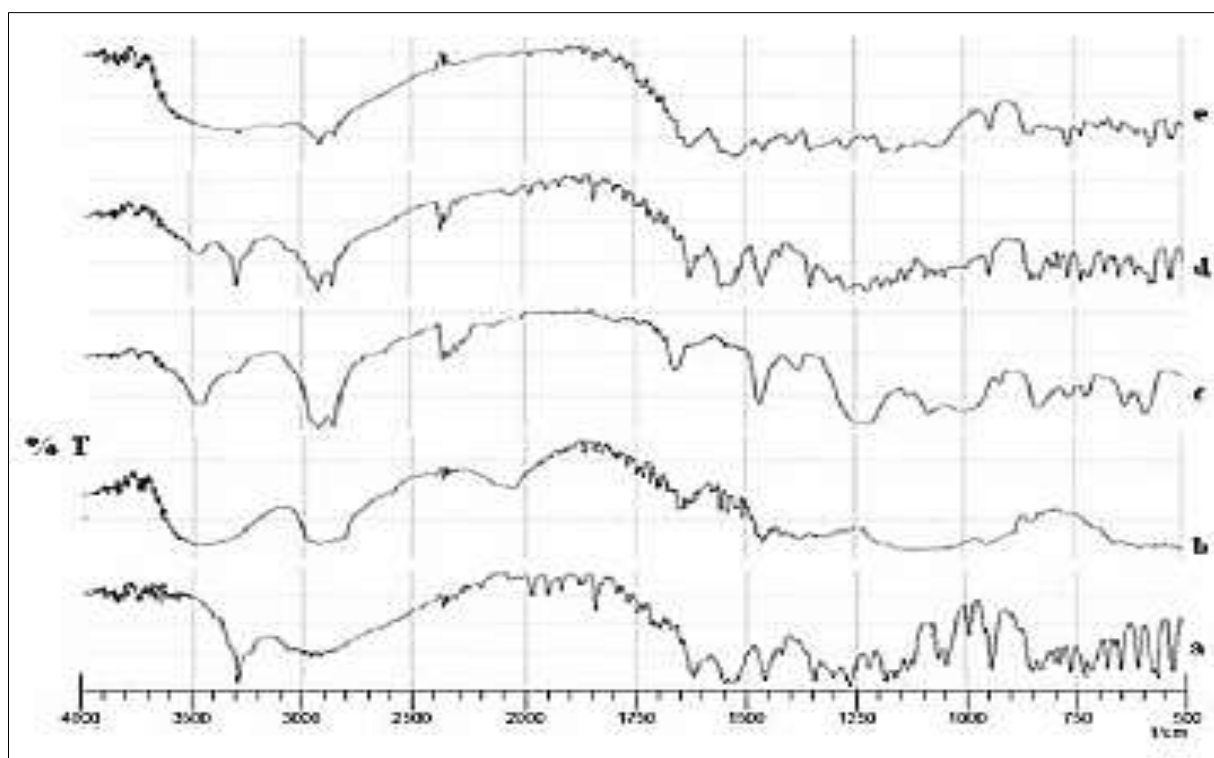


**Fig 16:** IR Spectra of a) Pure Meloxicam, b) HPMC E5, c) SDS, d) Physical Mixture and e) Spray Dried Nanoparticles

### FTIR Study

Spectrum of MLX, HPMC E5, SDS, physical mixture, and optimized formula of nanosuspension compared in the range of  $4000\text{--}500\text{ cm}^{-1}$ . In the present study, the interaction between MLX and stabilizers (HPMC and SDS) resulted in noticeable changes in the FT-IR spectra. The spectrum of MLX displayed characteristic peaks at  $3291.3$  and  $1622.02\text{ cm}^{-1}$  (N-H stretching),  $1591.16\text{ cm}^{-1}$  (C-O stretching),  $1163$  (S=O stretching) and  $1615.27\text{ cm}^{-1}$  (C=N stretching). In the case of HPMC E5, a sharp absorption at  $3471.63\text{ cm}^{-1}$  was due to the free O-H stretching (Raval and Patel, 2011) [29].

### Saturated Solubility

**Table 2:** Saturated solubility

Sample	Saturated solubility ( $\mu\text{g/mL}$ )
MLX	$4.4 \pm 0.50$
PM	$5.83 \pm 0.62$
Batch SHD	$21.84 \pm 0.78$

The aqueous solubility of MLX was improved greatly. The saturation solubility of nano-sized MLX ( $21.84\text{ }\mu\text{g/mL}$ ) was fourtimes greater than that of raw MLX ( $4.4\text{ }\mu\text{g/mL}$ ). The

reduction of the particle size of MLX to nano scale increased surface area and enhanced hydrophilicity which were responsible for the significantly increased saturation solubility (Raval and Patel, 2011)<sup>[29]</sup>.

### In vitro drug release

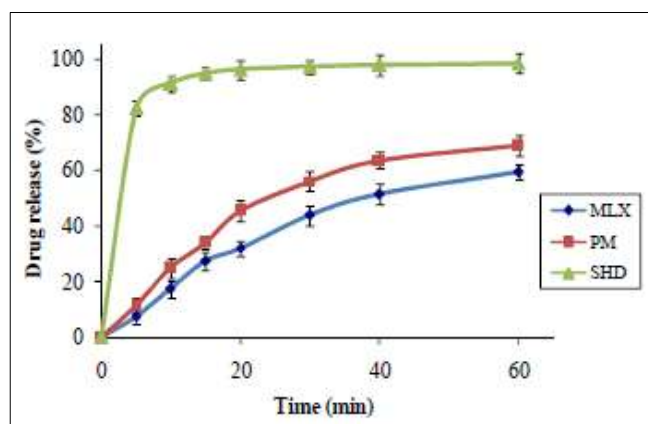


Fig 17: In vitro drug release of Meloxicam

Nano-sized MLX displayed a dramatic increase in the rate and extent of dissolution in comparison with raw MLX especially during the initial stage (first 5 min). SHD exhibited 82.59% drug dissolution within 5 min whereas only 7.43% of raw MLX dissolved during the same period. After 10 min, SHD was almost dissolved completely but only 17.39% of raw MLX had dissolved owing to its crystalline nature and larger crystal size. The dissolution profile of PM was all the more similar to that of raw MLX which showed that the mechanical physical mixing of raw MLX and stabilizers had little effect on the dissolution of raw MLX (Raval and Patel, 2011)<sup>[29]</sup>.

### Aspirin loaded albumin nanoparticles

Aspirin loaded Bovine serum albumin nanoparticles of sizes 46.8 nm to 190.8 nm were prepared by varying the aspirin protein ratio from 0.06 to 1.0. These particles were stable as

indicated by their zeta potentials and uniform characterized by low polydispersity (0.005 to 0.281). *In vitro* release kinetics study shows that aspirin loaded albumin nanoparticles are capable of releasing the drug in a slow sustained manner (almost 90% release at the end of 72 hrs). Aspirin loaded albumin nanoparticles are promising agents for regional drug delivery in inflammatory conditions of joints or thromboembolic manifestations of eye like diabetic retinopathy (Das *et al.*, 2005)<sup>[30]</sup>. Etodolac-loaded Poly Lactide Co – Glycolide (PLGA) nanoparticles might provide a promising carrier system for the effective delivery of this anti-inflammatory drug (Cirpanli *et al.*, 2009)<sup>[31]</sup>. The keterolac silica nano materials 1 : 8 sample showed a sustained release over ten hours; 90% of the drug was delivered at the end of the time (Goerne *et al.*, 2013)<sup>[32]</sup>. The dose-dependent analgesic effect of aerosolized ibuprofen studied in comparison with the oral treatment. The dose for aerosol treatment is three to five orders of magnitude less than that required for oral treatment at the same analgesic effect in mice (Makhmalzadeh *et al.*, 2009)<sup>[33]</sup>.

### Nanofiber Piroxicam

#### Estimation of drug content

Nanofibers equivalent to 20 mg of piroxicam were weighed and dissolved in 0.1N methanolic HCl and the absorbance was measured at 333 nm

#### Dissolution profile of nanofibers in 0.1N HCl

The *in vitro* dissolution studies were done to compare the rate of dissolution of these prepared drug loaded nanofibers with that of the pure drug. The test was performed in the United States Pharmacopeia Convention USP paddle apparatus using 900 ml of 0.1 N HCl (pH 1.2) at 37±0.5 °C and 50 rpm. Aliquots of 5 ml were withdrawn at various time intervals of 5, 10, 20 and 30 min and analyzed by UV spectrophotometer at 333 nm (Begum *et al.*, 2012)<sup>[34]</sup>.

### FTIR

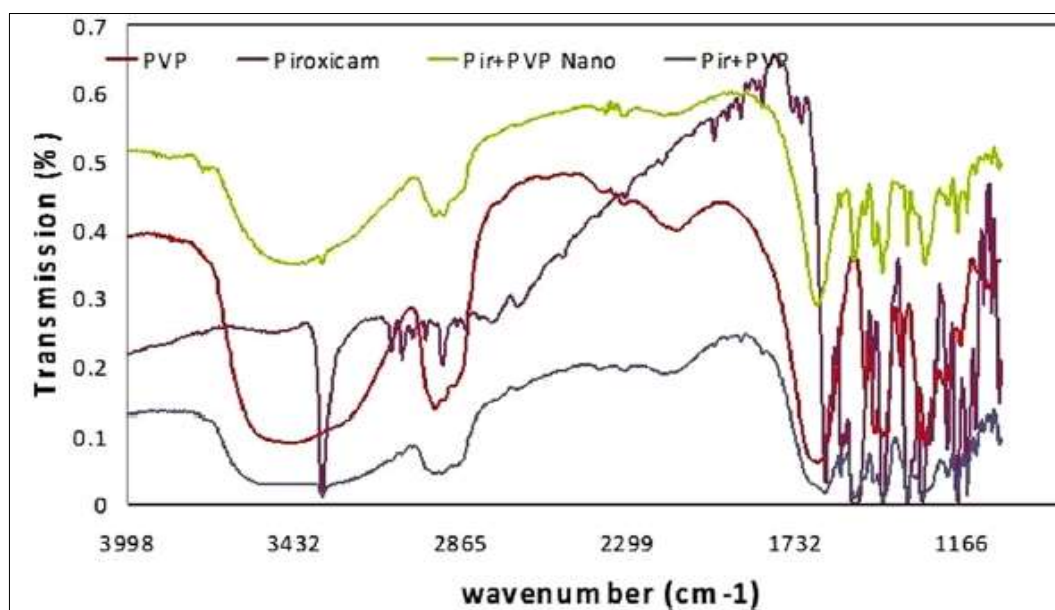
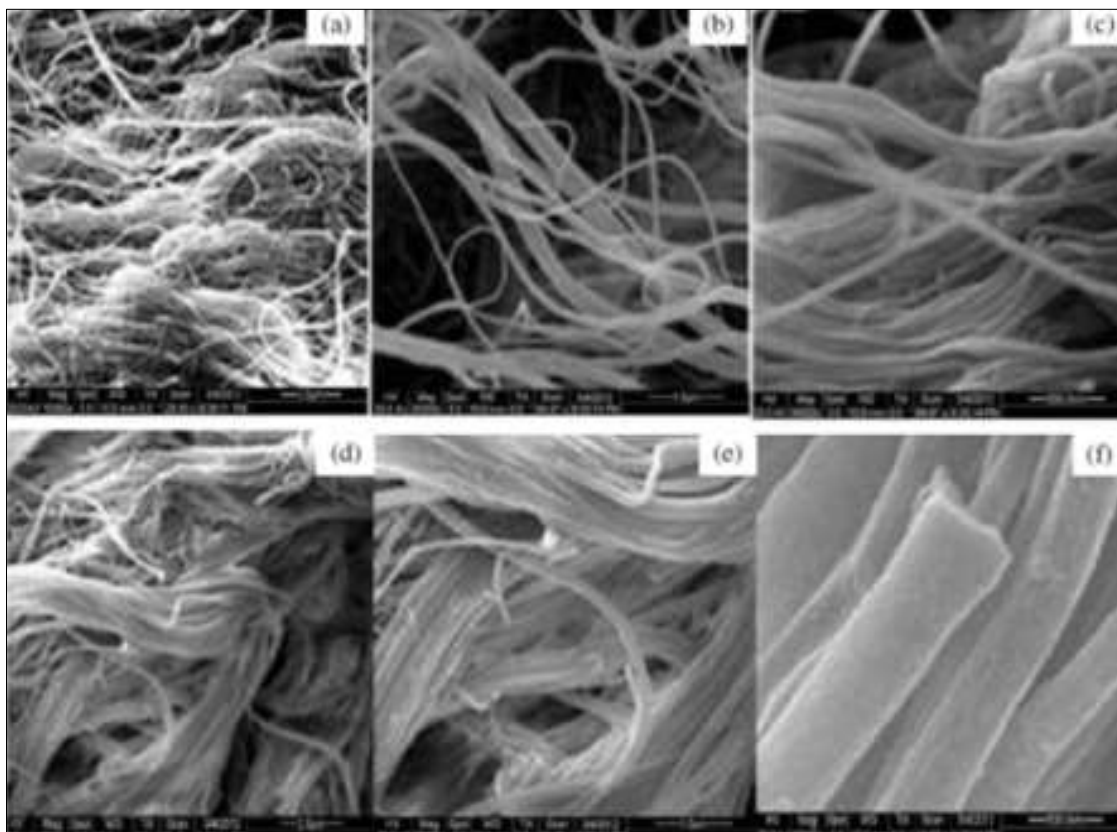


Fig 18: FTIR spectra of drug and drug loaded polymer

FTIR spectra were obtained on a Bruker spectrometer equipped with a DTSG detector. Samples were prepared in KBr discs. A polystyrene filter was used to check the spectrophotometer calibration. The N–H or O–H stretching vibration of piroxicam occurred at 3391 cm. The position and shape of this peak were not changed after treating piroxicam by PVP. This result suggested that in the absence of PVP, piroxicam remained in the same crystal structures. Piroxicam structure might exist as a mixture of tautomeric keto, enol or zwitterionic form. Due to the lack of a normal absorption of conjugated ketone in the recorded FTIR spectrum, piroxicam would be present as enol or zwitterionic form. Interestingly, the drug-PVP solid dispersion showed no peak of this N–H or

O–H stretching vibration. Comparing with piroxicam and physical mixtures, these peaks of solid dispersions were shifted toward lower wave numbers, indicating the presence of intermolecular hydrogen bonds between piroxicam and PVP. In drug-PVP solid dispersion with the drug:polymer ratio of 1:4 intermolecular hydrogen bond might be stronger than the others, therefore, the N–H or O–H stretching might be weakened, resulting in a weak and broad peak that was completely covered by bond stretches from PVP (Begum *et al.*, 2012) [34].

## SEM



**Fig 19:** SEM images of drug-loaded nanofibers (a, b), PVP (c) and PVP with piroxicam in increasing magnifications (d, e, f).

They were mounted directly on to the SEM sample stub using double-sided sticking tape and coated with gold film (thickness 200 nm) under reduced pressure (10–4 mm of Hg). Uniform fibers were obtained with average diameter of 600 nm. Piroxicam crystals were not detected by electron microscopy, indicating uniform distribution of drug and polymer solution. The nanofiber diameter is large and can be decreased by further optimizing the parameters used for the electrospinning process (Begum *et al.*, 2012) [34].

PVP used in the preparation of nanofibers, as it acts as a hydrophilic carrier, thereby enhancing the dissolution rate of the drug. The release rate of piroxicam-PVP nanofiber dissolution was twice increased as compared with the pure drug. A new drug delivery system for piroxicam, a non-steroidal anti-inflammatory drug (NSAID), was developed (Begum *et al.*, 2012) [34].

## Ibuprofen

Ibuprofen loaded fibers were prepared by using 10% (w/v) PVP 360 (Mw = 36 000 Da), 10% PVP / 2% SA (Sodium alginate) and 10% PEO (Polyethylene oxide) (Mw = 40.000 Da) / 2% SA as carrier polymers. 1% (w/v) drug polymer solutions used for spinning. Electrospinning was performed with a flow rate of 0.3 ml/h, a spinneret to distance of 15 cm, and an accelerating voltage of 20 kV. Sodium Ibuprofen was successfully loaded into nanofibers without altering its structure, as proven by UV spectra, FTIR and NMR. The fibers were found to be uniform in size and shape. Drug release from the fibers was studied in realistic *in vitro* conditions, and an interesting two-stage release mechanism observed for PEO- Sodium ibuprofen fibers (Makhmalzadeh *et al.*, 2009) [33].



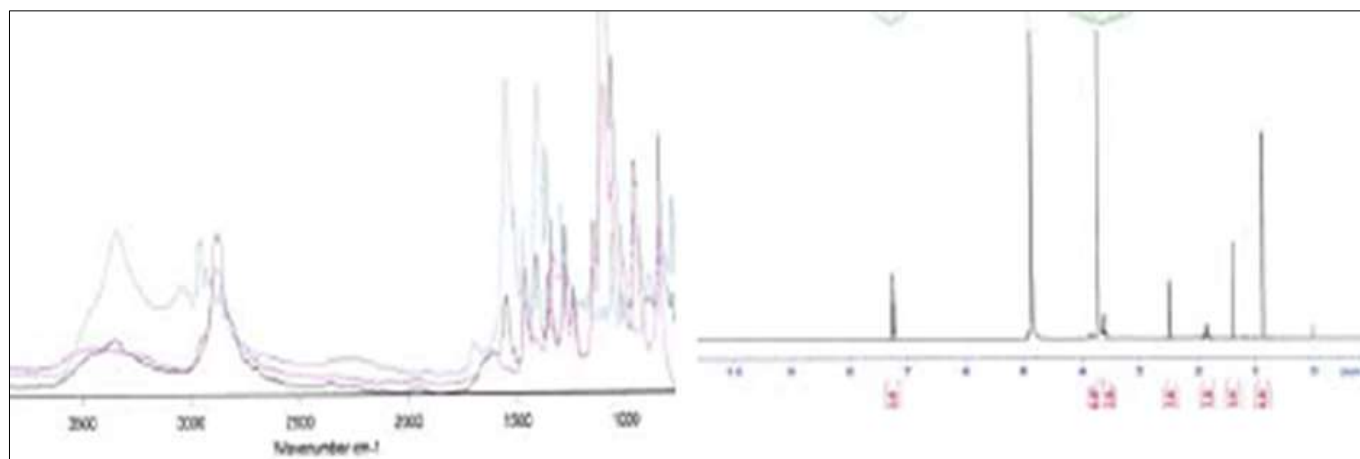


Fig 20: NMR spectrum of PEO-SA with sodium ibuprofen

FTIR spectra confirmed successful incorporation of ibu into the fibers, but also showed small shifts in the positions of the characteristic absorbances. The peaks shift suggest that interactions such as H-bonding existed between ibuprofen and the polymers (Makhmalzadeh *et al.*, 2009) [33]. XRD patterns showed that none of crystalline peaks of the drug were exhibited by the fibers, suggesting that ibu exists in an amorphous form in the fibers, and that the fiber components are mixed at the molecular level (Makhmalzadeh *et al.*, 2009) [33].

A dissolution study in an acetate buffer, the release of ibu from PVP nanofibers was very fast. The PVP-SA fibers released more slowly, and the PEO-SA nanofibers displayed the slowest release. The PVP nanofibers dissolved within 30s

and released all the encapsulated drug. The PVP-SA nanofibers liberated 100% of the incorporated drug after 5min. The PEO-SA nanofibers floated for one hour then sank and started dissolving. During the first 60 min the drug release rate was slow and reached a plateau at 13.6%. After 60 min, drug release accelerated and peaked after 127 min, where 100% of the drug had been released. The drug release was faster in SIF. The PVP nanofibers dissolved entirely with one minute. After 10 min, 60% of the drug was released from the PEO-SA nanofibers; nevertheless, more than 40% of the drug load stayed in the nanofibers (Makhmalzadeh *et al.*, 2009) [33].

#### SEM result

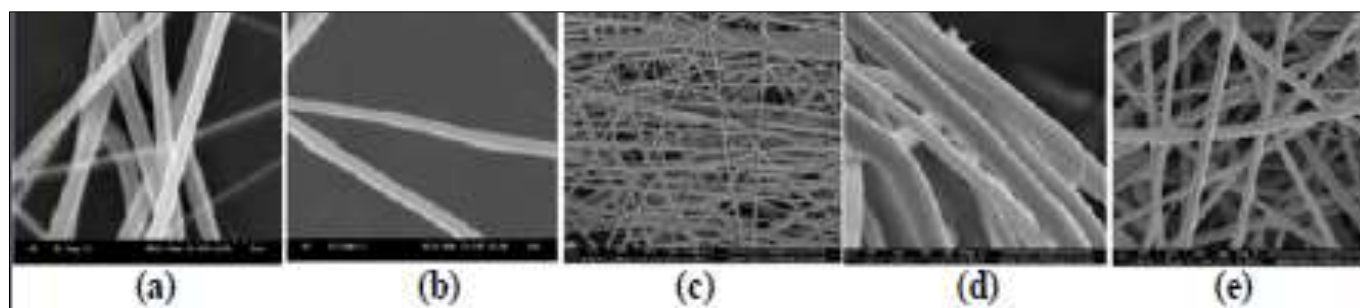


Fig 21: SEM images of the nanofibers. PVP; b) PVP-Ibu; c) PEO-SA-Ibu; d) PVP-SA; e) PVP-SA-Ibu

All the fibers with had smooth surfaces and cylindrical shapes. The fiber diameters for pure PVP and PVP-ibufibers were around 450nm. SEM images showed that all the fibers with had smooth surfaces and cylindrical shapes. The fiber diameters for pure PVP and PVP-ibufibers were around 450nm (Makhmalzadeh *et al.*, 2009) [33].

#### Indomethacin

Combination of Poly(meth)acrylate (Eudragit RS and Eudragit S) for prepration of nanofibers containing indomethacin using electrospinning method The optimized formulations were capable of drug loading up to 66% used for colonic delivery of indomethacin (Akhgari *et al.*, 2013) [35].

#### Compatibility of Nanofiber Components FTIR spectrum

The spectrum of indomethacin showed bands characteristic of

secondary carbonyl groups (C=O) at  $1714\text{ cm}^{-1}$ , (C=O amid) in  $1690\text{ cm}^{-1}$ , phenyl groups (C=C stretch vibration) at  $1523\text{ cm}^{-1}$  and (O-H stretch vibration) at  $3022\text{ cm}^{-1}$  (Akhgari *et al.*, 2013). The spectrum of ERS had a broad band characteristic of groups carbonyl (C=O) at  $1723\text{ cm}^{-1}$ , and ester linkages (C-O stretch vibration) at  $1149\text{ cm}^{-1}$ . The spectrum of ES showed a broad band characteristic of carbonyl groups (C=O) at  $1727\text{ cm}^{-1}$ , characteristic bands of hydroxyl groups (C-H stretch vibration) at  $2957\text{ cm}^{-1}$ . Two other spectra at  $1152$  and  $3087\text{ cm}^{-1}$  were also indicative of C-O and O-H stretch vibration, respectively. FTIR of formulation F1 exhibited the same spectra which in result there would be no significant shift in spectra and interactions between drug and polymer was not seen (Akhgari *et al.*, 2013) [35].



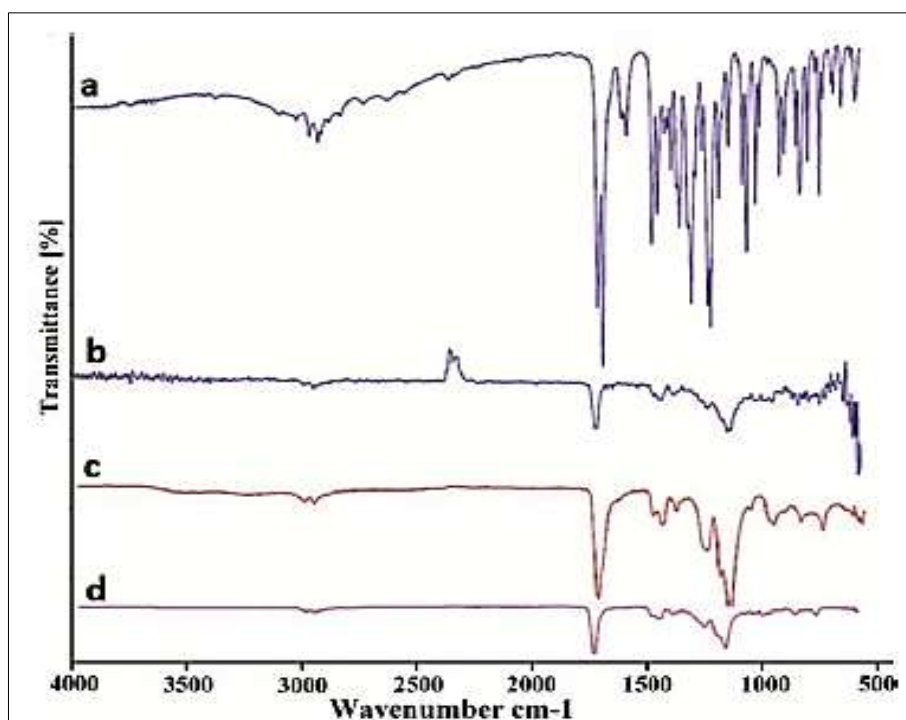


Fig 22: FTIR spectra(a) Indomethacin, (b) Eudragit RS, (c) Eudragit S, and (d) formulation F1

Meloxicam -loaded electrospun Poly Vinyl Alcohol mats as transdermal therapeutic agents. The fibers had average diameters ranging between 120 and 180 nm (Ngawhirunpat *et al.*, 2009) [36]. Lidocaine loaded nanofibers can provide an easy, practical and safe means of achieving effective postlaminectomy analgesia in rats (Tseng *et al.*, 2013) [37].

### Nanoemulsion

#### Aceclofenac Nanoemulsions for Transdermal Delivery: Stability and *In-vitro* Evaluation

Aceclofenac, Caprylic/capric triglyceride polyethylene glycol-4, complex (Labrafac®), caprylocaproyl macrogol-8-glyceride (Labrasol®), polyglyceryl-6-dioleate were considered for study.

#### *In vitro* Skin Permeation Studies

*In vitro* skin permeation studies were performed on a Franz diffusion cell with an effective diffusional area of 0.636 cm<sup>2</sup> and 4 mL of receiver chamber capacity using rat abdominal skin. The automated transdermal diffusion cell sampling system (SFDC6, Logan Inst, Avalon, NJ) was used for these studies. The full thickness rat skin was excised from the abdominal region, and hair was removed with an electric clipper. The subcutaneous tissue was removed surgically, and the dermis side was wiped with isopropyl alcohol to remove adhering fat. The cleaned skin was washed with distilled water and stored in the deep freezer at -21 °C until further use. The skin was brought to room temperature and mounted between the donor and receiver compartment of the Franz diffusion cell, where the stratum corneum side faced the donor compartment and the dermal side faced the receiver. Initially the donor compartment was empty and the receiver chamber was filled with ethanolic phosphate buffered saline (PBS) pH 7.4 (20:80% vol/vol). The receiver fluid was stirred with a magnetic rotor at a speed of 600 rpm, and the assembled apparatus was placed in the Logan transdermal permeation apparatus and the temperature maintained at 32 °C

± 1 °C. All the ethanolic PBS was replaced every 30 minutes to stabilize the skin. It was found that the receiver fluid showed negligible absorbance after 4.5 hours and beyond, indicating complete stabilization of the skin. After complete stabilization of the skin, 1 mL of nanoemulsion formulation (20 mg/mL aceclofenac) or 1 g of CG (20 mg/g) was placed into each donor compartment and sealed with paraffin film to provide occlusive conditions. Samples were withdrawn at regular intervals (0.5, 1, 2, 3, 4, 5, 6, 7, 8, 9, 10, 12, 20, 22, and 24 hours), filtered through a 0.45- membrane filter, and analyzed for drug content by UV spectrophotometer at  $\lambda_{max}$  of 274 nm (Chary and Katakam, 2011) [26].

The formulation F1 provided the highest release as compared with the other nanoemulsion formulations. The formulation F1 was also converted into nanoemulsion gel formulations by adding 1% wt/wt Carbopol 940 and was coded as NG1. The skin permeation profile of the optimized nanoemulsion formulation was compared with nanoemulsion gel (NG1) and CG using the Dunnett test of 1-way analysis of variance (ANOVA) (Chary and Katakam, 2011) [26].

#### *In vivo* Efficacy Study

The anti-inflammatory and sustaining action of the optimized formulation F1 was evaluated by the carrageenan-induced hind paw edema method in rats (Winter *et al.* 1995) [27].

The anti-inflammatory and sustaining action of the optimized formulation was evaluated by the carrageenan-induced hind paw edema method developed by Winter *et al.* in female Wistar rats. The percent inhibition value after 24 hours of administration was found to be high for F1— that is, 82.2% as compared with 41.8% for CG; this difference was extremely significant ( $p < .01$ ). The percent inhibition value for formulation NG1 was 71.4% (Figure 5), and the difference between F1's and NG1's percent inhibition was significant ( $p < .05$ ). The enhanced anti-inflammatory effects of formulation F1 could be due to the enhanced permeation of aceclofenac through the skin (Chary and Katakam, 2011) [26].

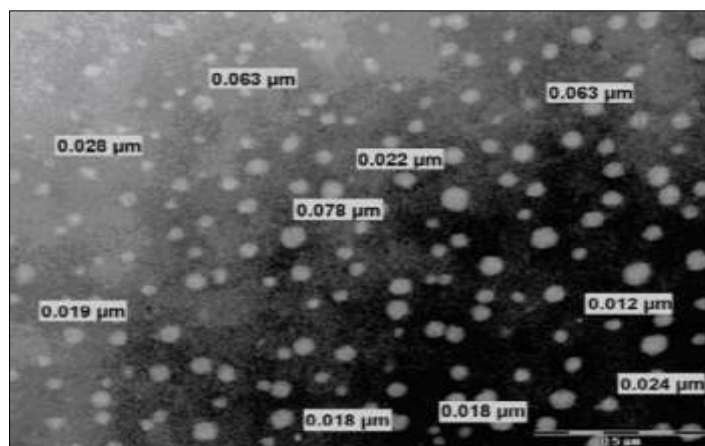


**Fig 23:** Transmission electron microscopy findings

In the TEM positive image, the nanoemulsion appeared dark and the surroundings were bright. Some droplet sizes were measured, as TEM is capable of point-to-point resolution. These sizes were in agreement with the droplet size distribution measured using photon correlation spectroscopy (Chary and Katakam, 2011) [26].

**Indomethacin**

**Antiinflammatory effects**

The enhanced anti-inflammatory effects of true nanoemulsions could be due to the enhanced permeation of indomethacin through the skin (Shakeel *et al.*, 2009).

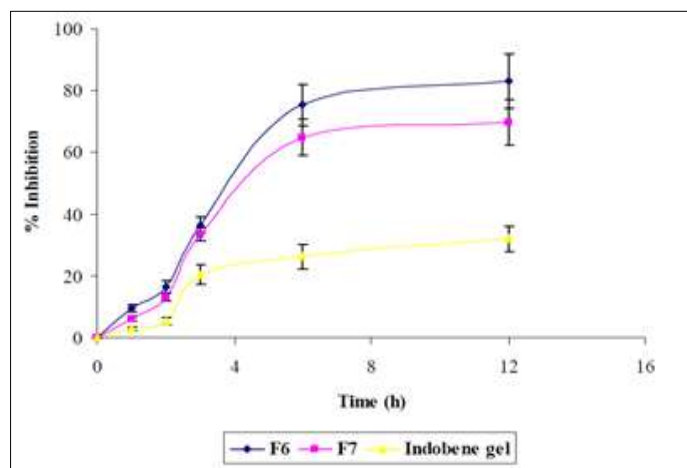


**Fig 24:** Anti-inflammatory effects of true nanoemulsion (F6), true nanoemulsion (F7) and marketed Indobene gel in Wistar male rats

**Celecoxib**

***In vitro skin permeation studies***

*In vitro* skin permeation was the highest in formulations T1 and T2 and the lowest for CXB gel

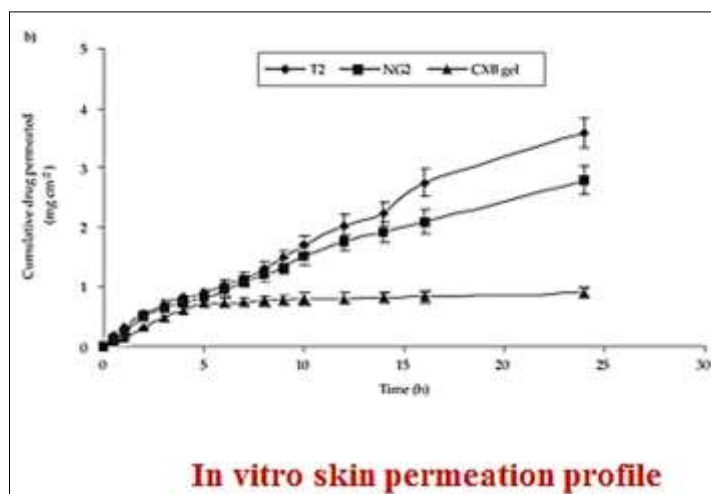


**Fig 25:** *In vitro* skin permeation profile of T1, T2 and CXB.

### Anti inflammatory Effects

The enhanced anti-inflammatory effects of formulation T2 could be due to the enhanced permeation of CXB through the skin. (Winter *et al.*, 1965) [27].

Nano emulsions can be used as potential vehicles for improved transdermal delivery of indomethacin as an approach to eliminate the side effect of the oral dose (Barakat *et al.*, 2011) [38]. Acrylate polymeric nanosuspensions of ibuprofen, flubrifrofen and cloricromene in ophthalmic delivery in the eye infection (Pignatello *et al.*, 2011) [39]. Ibuprofen traditional and novel nanoemulsion Formulations used as drug delivery through Rat Skin (Makhmalzadsh *et al.*, 2012) [33].

### Nanogel

The aceclofenac nanogel form represents an effective and better carrier for the transdermal/topical preparations. Nanogel formulation showed the better penetration in the skin may be due to the enhanced contact between the drug and the skin resulting from more surface area and hydration. The formulation showed stability over the study period and showed substantial increase in the efficacy in animal studies (Modi and Patel, 2011) [40].

### Antiinflammatory Effects

The % inhibition of the edema occurred to each group was calculated from the data of volume of paw, measured by plethysmometer (mercury displacement method). The paw volume was noted at 0, 0.5, 1, 1.5, 2, 3, 5 and 6 hours from the induction of the edema. Volume of inflamed paw goes on decreasing as time increases that shows drug acting on inflammation cause by Carrageenan. Optimized nanogel showed significant reduction in paw volume as compared with the control as well as standard group. The formulation showed not only decreased the inflammation to the larger magnitude, but also sustained this magnitude for the period of measurement. The results of anti-inflammatory activity were expressed as mean % inhibition rate of edema (n = 3). Statistical difference between the means were calculated using one-way analysis of variance (ANOVA) by Dunnett's test.

### Conclusion

Polymeric drug delivery systems are proven to have enhanced advantages compared to conventional NSAIDS drugs in enhancing therapeutic efficacy, fewer toxic effects, ease of making and handling. Nanomaterials like nanoparticle, nanofiber, nanoemulsion and nanogel used for the delivery of drugs out of these nanoemulsion and nanogel now used for the therapeutic purposes. Lack of sufficient data and guidelines regarding safe use of these nanomaterials in drug delivery. Safety, toxicity hazards, bioethical issues, physiological and pharmaceutical challenges get to be resolved in future.

### References

1. Abramson SB, Attur M, Amin AR, Clancy R. Nitric Oxide and inflammatory mediators in the perpetuation of osteoarthritis. *Current Rheumatology Reports*. 2001;3:535-541.
2. Hamor GH. Principles of Medicinal Chemistry Penn: Lea & Febiger, Philadelphia, 1989, 3<sup>rd</sup> 15:30
3. Lewis AJ Frust DW. Nonsteroidal Anti-inflammatory

4. Davis NM, MacLachlan AJ, Day RO, Williams KM. Clinical Pharmacokinetics and Pharmacodynamics of celecoxib: a selective cyclooxygenase2 inhibitor. *Clinical Pharmacokinetic*. 2000;38:225-242.
5. Jain NK. Pharmaceutical Nanotechnology, Sagar, Dr. Hari Singh Gour University, 2007. Mansoori GA, Rohani TB, Ahmadpour AZ, Eshaghi. Environmental Application of Nanotechnology, Annual Review of Nano-Research. 2008;2(2):2.
6. Mansoori GA. Principles of Nnotechnology. World Sci Pub Co, Hackensack, NJ; c2005.
7. Heyneman CA, Lawless-Liday C, Wall GC. Oral versus dermal NSAIDs in rheumatic diseases. *Drugs*. 2000;60(3):555-574.
8. Hooper L, Brown TJ, Elliott R, Payne K, Roberts C. The effectiveness of five strategies for the prevention of gastrointestinal toxicity induced by non-steroidal anti-inflammatory drugs: systematic review. *British Medical Journal* 2004;329:948.
9. Brune K, Hin ZB. The discovery and development of anti-inflammatory drugs. *Arthritis & Rheumatology*. 2004;50(8):2391-2399.
10. Marnett LJ. The COXIB experience: a look in the rearview mirror. *Annual Review of Pharmacology and Toxicology*. 2009;49:265-290.
11. Patrono C, Rocco B. Non-steroidal anti-inflammatory drugs: past, present and future. *Pharmacological Research*. 2009;59(5):285-289.
12. Zhang L, Gu FX, Chan JM. Nanoparticles in medicine: therapeutic applications and developments. *Clinical Pharmacology & Therapeutics*. 2008;83(5):761-769.
13. Semete B, Kalombo L, Katata L, Swai H. Nano-drug delivery systems: Advances in TB, HIV and Malaria treatment', Medicine, VBRI 2010 Press. ISBN: 978-81-920068-01.
14. Kubik T, Bogunia-Kubik K, Sugisaka M. Nanotechnology on Duty in Medical Applications 2005.
15. Poole PC and Frank J. Owens. Introduction to Nanotechnology. John Wiley & Sons, Inc 2003;07935:470-479.
16. Ramakrishna S, Fujihara K, Teo WE, Yong T, Ma Z, Ramaseshan R. Electrospun Nanofibers: Solving global issues. *Science Direct*. 2006;9(3):40-50.
17. Kattamuri SBK, Potti L, Vinukonda A, Bandi V, Chagantipati S, Mogili RK. Nanofibers in Pharmaceuticals- A Review. *American Journal of Pharm Tech Research*. 2012;2(6):187-212.
18. Shafiq S, Faiyaz S, Sushma T, Ahmad FJ, Khar RK, Ali M. Design and development of oral oil in water ramipril nanoemulsion formulation: *in vitro* and *in vivo* evaluation. *Journal of Biomedical and Nanotechnology*. 2007;3(1):28-44.
19. Shafiq S, Faiyaz S, Sushma T, Ahmad FJ, Khar RK, Ali M. Development and Bioavailability assessment of ramipril nanoemulsion formulation. *European Journal of Pharmaceutics and Biopharmaceutics*. 2007;66(2):227-243.
20. Kemken J, Zieger A, Muller BW. Influence of supersaturation on the pharmacodynamic effect of bupranolol after dermal administration using microemulsion as vehicle. *Pharmaceutical Research*.

- 1992;9:554-558. DOI: 10.1023/A:1015856800653
21. Kreigaard M. Dermal pharmacokinetics of microemulsion formulations determined by *in-vitro* microdialysis. *Pharmaceutical Research*. 2001;18:367-373. DOI: 10.1023/A:1011067300397
  22. Ochubiojo ME, Chinwude IO, Ibanga EA, Ifianyi SO. Recent Advances in Novel Drug Carrier Systems: Nanotechnology in Drug Delivery, In Tech, 2012, 84.
  23. Roullin VG, Callewaert M, Molinari M, Delavoie F, Seconde A, Andry MC. Optimised NSAIS-s loaded Biocompatible nanoparticles. *Nano-Micro Letters*. 2010;4:247-255.
  24. Lex TR, Rodriguez JD, Zhang L, Jiang W, Gao Z. Development of *In vitro* Dissolution Testing Methods to simulate Fed Conditions for Immediate Release Solid Oral Dosage Forms; c2022. DOI 10.1208/s12248-022-00690-5.
  25. Hoai NT, Quoc PT, Nam P, Dam LD, Nguyen TA, Nguyen TC, Chien DM. Ketoprofen encapsulated cucurbit[6]uril nanoparticles: a new exploration of macrocycles for drug delivery. *Advances in Natural Sciences: Nanoscience and Nanotechnology*. 2013;3(4):1-11
  26. Chary N. and Katakam P. Aceclofenac Nanoemulsions for Transdermal Delivery: Stability and *In-vitro* Evaluation., *Asian Journal of Pharmaceutical and Life Science*, 2011;1(4):355-369.
  27. Winter CA. Antiinflammatory testing methods: comparative evaluation of indomethacin and other agents. *NSAID*. 1965;82:190-202
  28. Landucci ECT, Antunes E, Donato JL, Faro R, Hyslop S, Marangoni S, *et al.* Inhibition of Carrageenin-induced rat paw oedema by crotapotin, a polypeptide complexed with Phospholipase A2. *British Journal of Pharmacology*. 1995;114(3):578-583.
  29. Raval AJ, Patel MM. Preparation and Characterization of Nanoparticles for Solubility and Dissolution Rate Enhancement of Meloxicam. *Material Science*. 2012;01(2):42-49.
  30. Das S, Banerjee R, Bellare Y. Aspirin loaded albumin nanoparticles by coacervation: Implications in drug delivery. *Trends Biomater. Artif. Organs*. 2005;18(2):203-212
  31. Çirpanli F, Robineau C, Çapan, Y, Çalış S. Etodolac loaded poly (lactide-co-glycolide) nanoparticles: formulation and *in vitro* characterization. *Journal of Faculty of Pharmacy of Ankara University*. 2009;29(2):105-114.
  32. Goerne TML, García MG, Grada R, Pérez OE, López G, Alvarez LM. Obtaining of sol-gel ketorolac-silica nanoparticles: characterization and drug release kinetics. *Journal of Nanomaterials*. 2013;8(1):1-9
  33. Makhmalzadeh BZ, Torabi S, Azarpanah M. Optimization of ibuprofen delivery through rat skin from traditional and novel nanoemulsion formulations. *Journal of Pharmaceutical Research*. 2012;11(1): 47-58
  34. Begum SK, Varma MM, Raju DB, Prasad PG, Phani AR, Jacob B. and Salins PC. Enhancement of dissolution rate of piroxicam by electrospinning technique. *Advances in Natural Sciences: Nanoscience and Nanotechnology*. 2012;3(1):1-4
  35. Akhgari A, Heshmati Z, Sharif B, Makhmalzade H. Indomethacin electrospun nanofibers for colonic drug delivery: Preparation and characterization. *Advanced Pharmaceutical Bulletin*. 2013;3(1):85-90
  36. Ngawhirunpat T, Panasopit P, Rojanarata T, Akkaramongkolporn T. Development of Meloxicam-Loaded Electrospun Polyvinyl Alcohol Mats as a Transdermal Therapeutic Agent. *Pharmaceutical Development and Technology*. 2009;14(1):70-79.
  37. Tseng YY, Liao JY, Chen WA, Kao YC, Liu SJ. Biodegradable poly (D,L)- lactide – co- glycolide) nanofibers for suitable delivery of lidocaine in to the epidural space after laminectomy. *Nanomedicine*. 2013;8(1):1-2
  38. Barakat N, Fouad F, Elmedany F. Formulation design of indomethacin-loaded nanoemulsion for transdermal delivery. *Pharmaceutic Analytica Acta*. 2011;21(2):2153-2435
  39. Pignatelli LR, Bucolo C, Puglisi G. Ocular tolerability of Eudragit RS100 and RL100 nanosuspensions as carriers for ophthalmic controlled drug delivery. *Journal of Pharmaceutical Science*. 2002;91(2):2636 - 41
  40. Modi J, Patel JK. Nanoemulsion Based Gel Formulation of Aclofenac for Topical Delivery. *International Journal of Pharmacy and Pharmaceutical Sciences*. 2011;1(1)6-12.